Available online at www.sciencedirect.com

SCIENCE DIRECT

Developmental Biology 280 (2005) 73–86

DEVELOPMENTAL BIOLOGY

www.elsevier.com/locate/ydbio

JNK signaling pathway required for wound healing in regenerating *Drosophila* wing imaginal discs

Manel Bosch[a], Florenci Serras[a], Enrique Martín-Blanco[b], Jaume Baguñà[a,*]

[a]*Departament de Genètica, Facultat de Biologia, Universitat de Barcelona, Diagonal 645, 08028 Barcelona, Spain*
[b]*Institut de Biologia Molecular de Barcelona, CSIC, Parc Científic de Barcelona, Josep Samitier 1-5, 08028 Barcelona, Spain*

Received for publication 20 May 2004, revised 23 December 2004, accepted 5 January 2005

Abstract

We have examined wound healing during regeneration of *Drosophila* wing imaginal discs fragments by confocal microscopy and assessed the role of components of the JNK pathway in this process. After cutting, columnar and peripodial epithelia cells at the wound edge start to close the wound through formation and contraction of an actin cable. This is followed by a zipping process through filopodial protrusions from both epithelia knitting the wound edges from proximal to distal areas of the disc. Activation of the JNK pathway is involved in such process. *puckered* (*puc*) expression is induced in several rows of cells at the edge of the wound, whereas absence of JNK pathway activity brought about by *hemipterous*, *basket*, and *Dfos* mutants impair wound healing. These defects are accompanied by lowered or loss of expression of *puc*. In support of a role of *puc* in wound healing, *hep* mutant phenotypes are rescued by reducing *puc* function, whereas overexpression of *puc* inhibits wound healing. Altogether, these results demonstrate a role for the JNK pathway in imaginal disc wound healing, similar to that reported for other healing processes such as embryonic dorsal closure, thoracic closure, and adult epithelial wound healing in *Drosophila*. Differences with such processes are also highlighted.

Keywords: *Drosophila*; Imaginal discs; JNK pathway; Wound healing; Regeneration

Introduction

After loosing body parts, several organisms are able to regenerate and restore the lost structures (see Ferretti and Geraudie, 1998, for general references). In *Drosophila*, the ability of imaginal discs to regenerate is well known (Bryant, 1975). When an imaginal disc is cut into two fragments and both are cultured in vivo prior to metamorphosis, one fragment regenerates the lost structures while the other produces a mirror-image duplicate of itself (Bryant, 1975; Schubiger, 1971). Such properties led in the 70s and 80s to a flurry of experimental manipulations, cutting wing and leg discs, to analyze the processes of wound healing, cell proliferation, growth, and pattern formation (Adler, 1984; Bryant and Fraser, 1988; Dale and Bownes, 1981, 1985; Dunne, 1981; Karlsson and Smith, 1981; Schubiger, 1973). Out of them, general models on pattern formation were proposed which formally accounted for a good deal of data from *Drosophila* and other regenerating systems (Bryant et al., 1981; French et al., 1976; Meinhardt, 1983).

Wound healing is the first necessary step for regeneration. Firstly, it is important to isolate the regenerate from the external media and to avoid intrusion of pathogens. And secondly, it is required to initiate growth and pattern formation (Bryant and Fraser, 1988). All imaginal discs in *Drosophila* are made up of two layers of epithelial cells. One layer, made by a highly columnar epithelium (CE) represents the disc proper and differentiates into adult structures during metamorphosis. Overlaying the CE, and connected to it, is a layer of flat, squamous cells, called the peripodial epithelium (PE), which has a leading role in disc eversion and thoracic closure (Agnès et al., 1999; Pastor-Pareja et al., 2004). Pioneer work by Reinhardt et al. (1977)

* Corresponding author. Fax: +34 93 4110969.
E-mail address: jbaguna@ub.edu (J. Baguñà).

0012-1606/$ - see front matter © 2005 Elsevier Inc. All rights reserved.
doi:10.1016/j.ydbio.2005.01.002

and Reinhardt and Bryant (1981), showed that both epithelia, namely the CE, bear a terminal web of microfilaments at the apical area, extending into the microvillar ridge, and connected with the zonula adherens which links the lateral cell surfaces throughout the CE. After wounding, the wound edges of both epithelia curl towards the lumen and the wound surface contracts, likely by the action of microfilaments. Short-lived cell contacts are first established between CE and PE (heterotypic contacts) to switch at 24 h to homotypic contacts bearing desmosomes between closely apposed CE cells along the wound (Reinhardt and Bryant, 1981). Using fluorescent cell markers, Bryant and Fraser (1988) studied the time course of wound healing in wing discs. After 24 h of culture, results showed that healing involved fusion of the two cut edges bringing together the cells along them. Interestingly, DNA synthesis, assessed by bromodeoxyuridine (BrdU) incorporation, was localized near the position of the wound from 18 h of culture on. Ensuing regeneration seemed, in agreement with the Polar Coordinate Model (Bryant et al., 1981; French et al., 1976), to result from intercalation of new structures derived from proliferating cells around the closed wound area.

These studies, however, did not specify the mechanisms by which wound healing actually occurs. During epithelium closure in epithelia other than imaginal discs, cells either migrate over a substrate such as the larval epidermal cells in disc eversion and thoracic closure (Agnès et al., 1999; Noselli and Agnès, 1999) or close the gap through push and pull forces exerted by leading edge cells and amnioserosa cells as in dorsal closure in *Drosophila* embryos (Glise and Noselli, 1997; Jacinto et al., 2000, 2002; Martin-Blanco et al., 1998). Experimental wound healing studies in *Drosophila* embryos have shown that an actin cable operates as a 'purse-string' to draw the hole close, whereas dynamic filopodia protrusions are essential for the final 'knitting' together of epithelial cells (Wood et al., 2002). In epidermal wound healing in *Drosophila* larvae, no actin cable was observed; instead, after clotting, epidermal cells spread along and through the plug led by lamellipodial extensions until epithelial continuity is reestablished (Galko and Krasnow, 2004). Finally, in epithelial wounds in adult *Drosophila* formation of an actin cable was not studied; however, cytoplasmic extensions from the cells of the wound, suggestive of lamellipodia or filopodia, were described. Such extensions allow cells to migrate towards each other under the melanin clot until the epidermis sutures (Rämet et al., 2002).

The spreading and migrating features of leading edge cells in embryonic dorsal closure and disc thoracic closure, as well as in experimental wound healing studies mentioned above are controlled, among others, by genes of the Jun-N-terminal Kinase (JNK) signalling pathway. JNK pathway mutants such as: *hemipterous* (*hep*) (Glise et al., 1995), *basket* (*bsk*), *Dfos* (also known as *kayak*; Zeitlinger and Bohmann, 1999; Zeitlinger et al., 1997) lead to dorsal open embryos or show severe defects in disc morphogenesis and thorax formation or incomplete wound healing. During dorsal and thoracic closure (Agnès et al., 1999; Jacinto et al., 2000, 2002; Martin-Blanco et al., 1998), as well as during larval and adult wound healing (Galko and Krasnow, 2004; Rämet et al., 2002), the JNK signalling pathway is selectively activated at the leading edge cells. Such cells could be specifically monitored through the expression of *puckered* (*puc*), a component of the JNK pathway. *puc* encodes a phosphatase that dephosphorylates and consequently inactivates MAPK family members, including JNKs (Martin-Blanco et al., 1998). Therefore, the level of JNK signalling is controlled by a *puc*-dependent negative feedback loop. In addition, its expression is reduced in JNK mutants (Glise and Noselli, 1997; Glise et al., 1995; Martin-Blanco et al., 1998) indicating that *puc* transcription is under the direct or indirect control of the JNK signalling pathway. In embryonic dorsal closure, *puc* expression is restricted to a single row of cells, whereas in disc thoracic closure and larval and adult wound healing, it is expressed in several rows. Taken together, these results suggest that *puc* expression might also be activated during wound healing of imaginal discs. If so, it may represent a very useful marker to monitor wound healing itself as well as the activation of the JNK signaling in processes other than embryonic dorsal and thoracic closure and larval and adult wound healing.

In this study, we describe wound healing in regenerating wing imaginal discs using confocal microscopy and specific cell markers. Differential behavior and cell shape changes in columnar epithelium (CE) and peripodial epithelium (PE) and the role of actin cables in gap closure were also studied. Finally, although epithelial closure in regenerating imaginal discs bear features not present in dorsal and thoracic closure and larval and adult wound healing, we tested whether *puc* is specifically expressed at the edges of the wound area and whether *puc* and by extension other members of the JNK pathway (*hep*, *bsk*, *Dfos*) are required in this process. We report that *puc* is induced in several rows of cells of the CE and PE along the wound, that JNK mutants inhibit wound healing and regeneration, and that the actual process of wound healing occurs by contraction of the actin cable followed by zippering together the epithelial edges of the wound in a disto-proximal direction.

Materials and methods

Drosophila stocks and genetics

A description of genetic markers and chromosome balancers used in this study can be found in FlyBase. The hep^{r75} allele is an imprecise excision of a P element insertion in the *hep* gene (Glise et al., 1995). $puc^{E69\text{-}A}$-*Gal4* and $puc^{E69\text{-}F}$-*Gal4* are P-*Gal4* insertions in the *puc* gene (Pastor-Pareja et al., 2004). Whereas $puc^{E69\text{-}A}$-*Gal4* shows a WT phenotype, $puc^{E69\text{-}F}$-*Gal4* insertion causes pupal

lethality in homozygous conditions. Fly cultures and crosses were grown on standard fly medium at 25°C.

Gal4 targeted expression

Targeted expression of UAS-driven transgenes was induced using an *en-Gal4* line (Brand and Perrimon, 1993). The *UAS*-driven transgenes are as described: *UAS-bsk^{DN}* (provided by D. Bohmann) and *UAS-puc2A* (Martin-Blanco et al., 1998). The *UAS-Dfos$^{N\text{-}Ala}$*, *UAS-Dfos$^{C\text{-}Ala}$*, *UAS-Dfos$^{pan\text{-}Ala}$* are different dominant negative (DN) forms generated by amino acidic substitutions at specific phosphorylation sites of *Dfos* (Ciapponi et al., 2001). The following crosses were performed: males *UAS-X* (all in the 3rd chromosome) were crossed to *en-Gal4; UAS-GFP* females. *X* represents any of the *UAS*-driven transgenes.

Imaginal disc manipulation

Wing imaginal discs were removed from mid-late third Instar larvae, 100–120 h after egg laying (AEL), into Schneider's insect medium (Sigma) and cut into the required fragments using electrolytically sharpened tungsten needles. In all experiments, 90° sectors were cut out from the disc to produce 3/4 fragments for study. To study wound healing, a 90° sector which includes the whole anteroventral compartment and the anterodorsal part of the wing pouch was cut out (see Fig. 1A) and the remaining 3/4 fragment analyzed. In overexpression experiments, we used discs from *en-Gal4; UAS-GFP* stock which allows to visualize the A/P boundary. 90° sectors were cut within anterior or posterior compartments close to the A/P boundary to generate 3/4 fragments with wound edges limited by anterior or posterior cells, respectively (see Figs. 5A, C). In all experiments, fragments were implanted, using the technique described by Ursprung (1967), into the abdomens of virgin Canton-S females which provide a perfect environment and infections are cleared. Implantation was performed using sharpened fine glass capillaries and implanted females kept at 25°C. Regenerating fragments were recovered at different times after implantation (5, 12, and 24 h, and 7 days).

For each experiment, several fragments were implanted and recovered. Recovered fragments with unclear morphology were discarded. Overall, after extraction from the abdominal cavity and staining, 65% of all implanted fragments were used which meant a minimum of 10 imaginal discs per experiment and time point.

Immunocytochemistry

Regenerating fragments were fixed in 4% paraformaldehyde on ice for 20 min and washed in PBS. Antibody incubation was performed using standard techniques with anti-FasciclinIII (a gift of Dan Brown), at 1:1000 dilution, to detect the cellular membrane, and anti-homothorax (provided by Richard Mann), at 1:1000 dilution, which specifically labels all cell nuclei of the discs, those in the wing pouch giving a weaker signal. To stain the actin cytoskeleton of whole discs and fragments, a Rhodamine-coupled phalloidin (Molecular Probes) was used at 1:40 dilution in PBS for 30 min after fixation (in 4% paraformaldehyde on ice).

After staining, samples were mounted on SlowFade Light Antifade kit (Molecular Probes) and analyzed with a Leica TCS 4D confocal microscope. Images were processed using the ImageJ (NIH Image; www.rsb.info.nih.gov/ij) and Photoshop 7.0 software (Adobe Corp).

Results

Description of the wound healing process

All fragments examined were healed at 24 h (Fig. 1). Immediately after cutting (Figs. 1B, C) the columnar epithelium (CE) and, to a lesser extent, the peripodial epithelium (PE) curve toward each other. This produces a temporal backward retraction of the wound edge which is more pronounced for the PE. At 5 h, a clear shortening of the wound edge (wound contraction) is observed (Figs. 1D, F, H) and PE cells at the edge show an actin-rich cable (Fig. 2A). Closer inspection at the wound vertex area (Figs. 1E, G, I, J) shows elongated peripodial cells leaning towards the CE. Meanwhile, CE cells have closed the gap by their basolateral surface (Fig. 1H), whereas their apical regions still remain open but zipping out with neighbor cells through filopodia extensions (Figs. 1G, 2B–D). At 12 h after cutting and implantation, a stricking shortening of the wound surface is observed (Figs. 1K, L M). Elongated PE cells cover the wound vertex and CE contracts easing the process of zipping, through filopodia extensions. At 24 h, the wound edges match together (Figs. 1N, O, P). PE cells are still elongated towards the wound tip and CE cells have zipped the wound (Figs. 1O, P). The extensive heterotypic contacts reported by Reinhardt et al. (1977) and Reinhardt and Bryant (1981) using transmission and scanning electron microscopy could not be ascertained using confocal microscopy. However, they are likely present at different stages of wound healing in those areas where both epithelia meet (see Fig. 1P).

Induction and expression of puc during wound healing in imaginal discs

The JNK signaling pathway (Fig. 3A) is an evolutionary conserved pathway, which in *Drosophila* controls the migration of epithelial cells during embryonic dorsal closure, disc thoracic closure, and larval and adult wound healing. Its best characterized upstream genes are *hemipterous* (*hep*) and *basket* (*bsk*), while downstream targets, like *Dfos* and *Djun*, control the localized expression of *puckered* (*puc*) and other effectors (e.g., *decapentaplegic*

(*dpp*) in embryonic dorsal closure). Therefore, if the JNK pathway also operates in wound healing and regeneration, we should expect that loss-of-function mutations and overexpression of dominant negative mutations of the pathway will impair them. In addition, overexpression of *puc*, a negative regulator of the pathway, would also have an inhibitory effect.

To test role of the JNK pathway in imaginal disc wound healing and regeneration, we first assayed the expression of its main down-stream effector, the gene *puckered* (*puc*). $puc^{E69\text{-}A}$*-Gal4* was assayed for GFP activity during wound healing of regenerating imaginal wing discs from $puc^{E69\text{-}A}$*-Gal4*; *UAS-GFP* flies. In uncut wing, imaginal discs $puc^{E69\text{-}A}$*-Gal4* is strongly expressed in the stalk region (Fig. 3B), where imaginal discs connect to the larval epidermis, as well as in rows of cells of the PE close to the CE. The WT pattern of *puc* expression is maintained throughout healing and regeneration (Figs. 3C, D, G, H, I).

puc is expressed at the wound of regenerating discs. Interestingly, it is not immediately detected after cutting. At 5 h, a few scattered positive cells for *puc* are seen in both

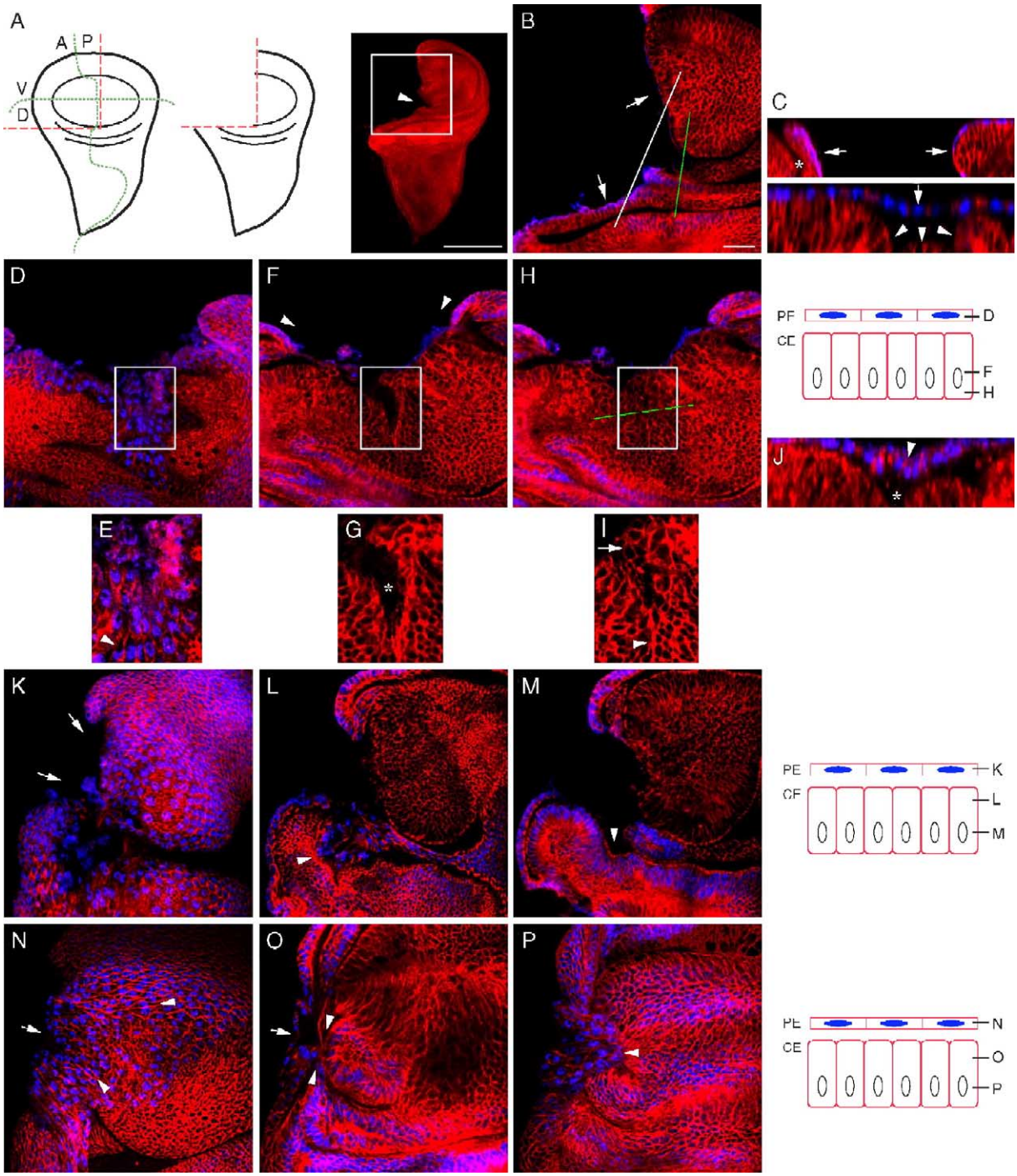

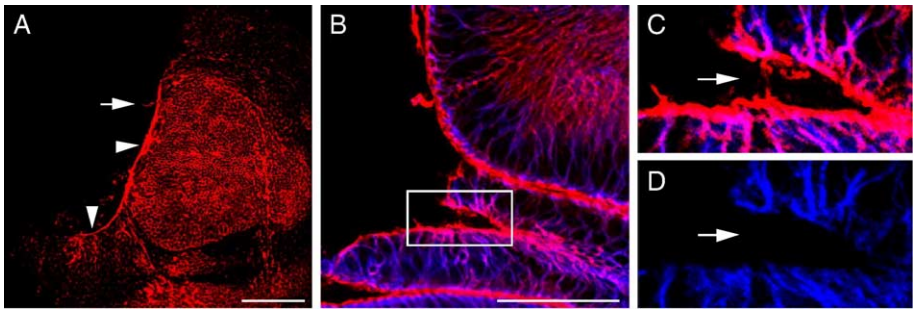

Fig. 2. Actin cytoskeleton during wound healing stained with phalloidin (red) for actin and Fasciclin III (blue) to delineate cell boundaries. (A) Projection of PE confocal planes at the wound edge of a 3/4 fragment after 5 h of in vivo culture. An actin cable is seen all along the peripodial edge (arrowheads) and filopodial protrusions are already visible (arrow). (B) CE confocal planes at the wound edge of a 3/4 fragment after 5 h of in vivo culture. Zippering is observed at the wound vertex (white square). (C, D) Enlargement of white square in (B). Filopodial protrusions are labeled with phalloidin (red) for actin (arrow in C), but not with Fasciclin III (arrow in D). Scale bar: 20 μm.

epithelia (Figs. 3D, E, F) spanning an average of 10 to 15 cell rows from the wound edge. By 12 h, the number of *puc*$^{E69\text{-}A}$*-Gal4;UAS-GFP*-positive cells reach a maximum, though its range is maintained to 10–15 rows of cells from the wound edge (Fig. 3G). Such increase occurs in both epithelia (Figs. 3J, K). Meanwhile, cells elongate towards the wound edge and the distal tips of the wound contracts, in parallel to maximal *puc*$^{E69\text{-}A}$ expression. At 24 h, the number of GFP cells has decreased, though its range still spans 10–15 rows of cells (Fig. 3H), and 3/4 fragments are almost completely healed. From then on, GFP expression persists around the healed wound up to 6–7 days of culture when regeneration is completed (Fig. 3I).

hep controls puc expression and puc suppresses hep phenotypes in imaginal disc wound healing

During embryonic dorsal closure, the JNK pathway activates *puc* expression at the leading edge of advancing ectodermal cells. *puc* expression initiates in turn a negative feedback loop that controls the levels of JNK activity (Glise and Noselli, 1997; Glise et al., 1995; Martin-Blanco et al., 1998). Such regulatory links also exist in disc thoracic closure during metamorphosis (Agnès et al., 1999) and in larval and adult wound healing (Galko and Krasnow, 2004; Rämet et al., 2002). To test if the JNK pathway also mediates *puc* induction during wound healing in regenerating imaginal discs, *puc* expression was analyzed in fly mutants of this pathway. Most mutations affecting dorsal closure cause embryonic lethality and no imaginal discs are produced. However, using the hypomorphic allele of *hemipterous* (encoding the MAPKK), *hep*^{r75}, dorsal closure is not impaired whereas wing disc fusion during thoracic closure is inhibited leading to pupal lethality. Wing discs from hemizygotic *hep*^{r75}*/Y* males (experimental) were cut and 3/4 fragments left to regenerate. 3/4 fragments from heterozygotic *hep*^{r75}*/FM7* females served as controls. At 24 h, over 85% of control fragments (n = 14) were healed or almost healed (Fig. 4A), whereas 3/4 fragments (n = 14) from *hep*^{r75}/Y discs showed an open wound (Fig. 4B) and no elongation of PE cells towards the wound edge (Fig. 4D). After 7 days, hemyzygous *hep*^{r75}/Y discs remained unhealed with no signs of regeneration (Fig. 4C). Statistical analysis using the Fisher exact test (Fisher, 1935) showed that there was a significant difference ($P < 0.05$) between *hep*^{r75}/Y and *hep*^{r75}*/FM7* genotypes.

puc expression in *hep*^{r75} 3/4 regenerating disc fragments was monitored using *puc*$^{E69\text{-}A}$*-Gal4;UAS-GFP* in *hep*^{r75}*/Y* males. At 24 h after cutting, the wound is partially contracted but unhealed (Fig. 4F). *puc* expres-

Fig. 1. Wound healing in wing imaginal disc fragments. (A) Left: wing imaginal disc showing the cutting lines (broken red line) used to generate a 3/4 fragment (center). Right, confocal image of a 3/4 fragment after cutting. Arrowhead points to the wound vertex. Anteroposterior (A/P) and dorsovental (D/V) compartment boundaries are represented by dotted green lines. Scale bar: 100 μm. (B) Higher magnification of the square in (A). Scale bar: 20 μm. Arrows indicate wound edges. For white and green lines, see (C). (C) Z confocal sections. Top (white line in B) shows the large gap separating the edges of the wound (arrows). Asterisk points to the hinge furrow. Bottom (green line in B) shows PE (arrow) and CE (arrowheads) cells at the wound vertex. (D, F, H) 3/4 fragments after 5 h of in vivo culture. (D) Confocal section 6 μm below the PE (see drawing at right). Peripodial cells cover the wound edge at the wound vertex (arrowhead). (E) Enlargement of the white square in D. (F) Confocal section at the CE focal plane. Epithelia at the wound tips (arrowheads) contract towards the vertex. (G) Magnification of the white square in (E) showing the non-healed region (asterisk). (H) Confocal section 3 μm below F (see drawing at right). CE cells have already closed the wound. (I) Higher magnification of the white square in (H). CE cells zipping the wound (arrow) are larger in size than those distant from the wound. Arrowhead points at the zipping line. (J) Z-section of green line in (H). PE cells (arrowhead) elongate to cover the vertex (asterisk). (K, L, M) 3/4 fragments after 12 h of in vivo culture. (K) Confocal section at the PE level (see drawing at right). Wound tips (arrows) have contracted substantially reducing the wound surface. (L) Confocal section 7 μm below (K) at the CE level. CE has contracted (arrowhead) and colocalize with PE cells. (M) Confocal section at the CE level 10 μm below (L). CE cells have contracted and zip the epithelium (arrowhead). (N, O, P) 3/4 fragments after 24 h of in vivo culture. (N) Confocal section at the PE level (see drawing at right). PE cells elongate (arrowheads) towards the wound edge (arrow). (O) Confocal plane at CE level, 10 μm below (N). PE cells (arrow) cover the wound and CE cells have zipped the wound (arrowheads). (P) Confocal section 8 μm below (O). PE cells elongate and enclose (arrowhead) the wound edge. In all confocal images, Fasciclin III (red) is used to delineate cell boundaries and *hth* (blue) to label cell nuclei. Drawings at the right hand side indicate the levels at which confocal sections were taken.

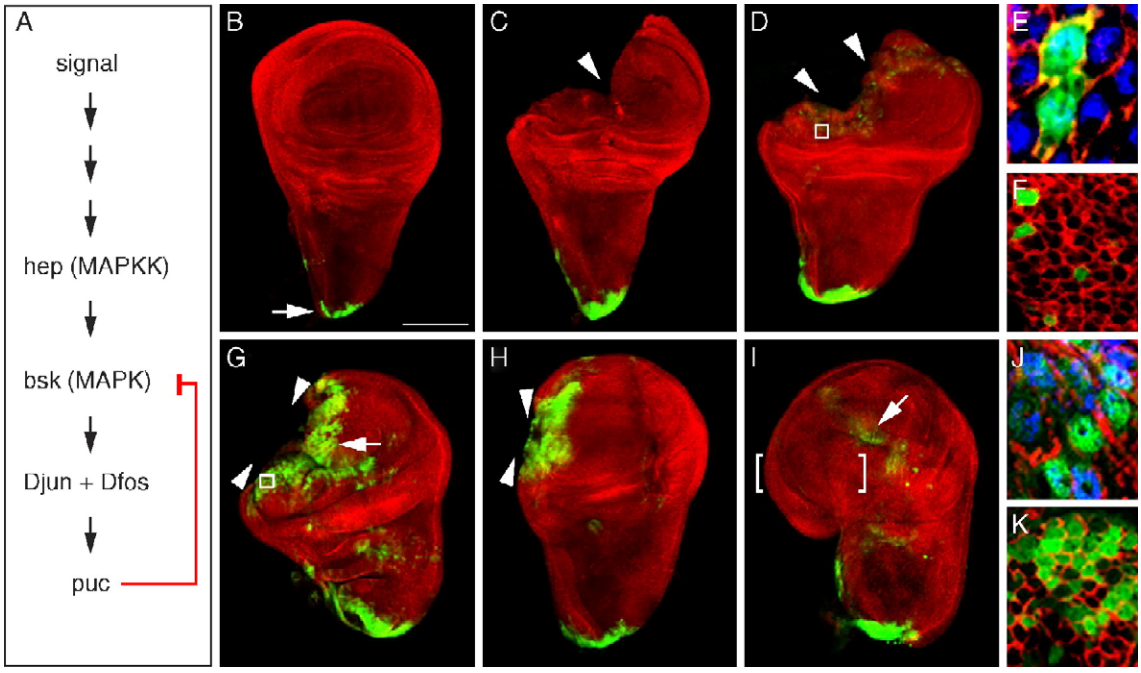

Fig. 3. *puc* expression patterns during imaginal disc wound healing. Double staining for *puc* (green; $puc^{E69\text{-}A}$*–Gal4;UAS-GFP*) and Fasciclin III (red). (A) Diagrammatic representation of the main components of the JNK signalling pathway in *Drosophila* studied in this work. For further details, see text. (B) Intact wing disc. *puc* expression at the stalk (arrow) holds along wound healing and regeneration. (C) 3/4 fragment immediately after cutting. *puc* is expressed at the stalk but not at the wound edge (arrowhead). (D) 3/4 fragment after 5 h of in vivo culture. *puc* is weakly detected within several rows of cells from the wound edge (arrowheads). (E) Enlargement of white square in (D) at the PE confocal plane. *puc* is expressed in a few PE cells. *hth* (blue) marks peripodial cells. (F) Magnification of square in (D) at the CE confocal plane. *puc* is expressed in a few scattered CE cells. (G) 3/4 wing disc fragment after 12 h in vivo culture. *puc* is strongly expressed at the wound edge (arrow) in parallel with wound contraction (arrowheads). (H) 3/4 fragment after 24 h of in vivo culture. *puc* is expressed at the wound (arrowheads) which is almost closed. (I) 3/4 fragment after 7 days of in vivo culture. A few cells express *puc* at the former wound region (arrow). The regenerated CE (bracketed) does not express *puc*. (J, K) Enlargement of square in (G). More PE cells (J) and CE cells (K) express *puc* than at 5 h. In all figures, except E, F, J, K, scale bar: 100 μm.

sion is present but in fewer cells than in 12 h (Fig. 3G) and 24 h (Fig. 3H) regenerating controls. To test whether the non-healing phenotype results from lower JNK activity, the $puc^{E69\text{-}F}$*-Gal4* strain, which inactivates *puc* function, was used. 3/4 fragments from hep^{r75}/Y flies with one dose of puc^{+} showed at 24 h increased levels of JNK activity and *puc* expression (monitorized by GFP) (Fig. 4G). Moreover, these fragments had the wound more closed. Closer inspection of the healed area shows curled wound edges (Fig. 4H) and PE cells elongating towards the wound (Fig. 4E). Interestingly, discs $puc^{E69\text{-}F}$*-Gal4;UAS-GFP* in hep^{r75}/Y background, showed a higher number of *puc*-positive rows of cells than controls.

Overexpression of dominant negative forms of basket and Dfos affects wound healing through the JNK pathway

Since *Djun*, *bsk*, and *Dfos* are targets of the JNK pathway downstream of *hep*, they are likely to be switched on and needed during imaginal disc wound healing. To test it, we overexpressed a *UAS* dominant negative form of *bsk* ($UAS\text{-}bsk^{DN}$) driven by *en-Gal4* in 3/4 regenerating fragments. Because *en* is expressed only in the posterior compartment, bsk^{DN} will also be expressed there. Two types of cuts were performed in discs of *en-Gal4*; $UAS\text{-}GFP/UAS\text{-}bsk^{DN}$ larvae. First, a 90° sector was cut within the anterior compartment giving 3/4 regenerating fragments in which the wound area is limited by anterior cells which do not express bsk^{DN} (Fig. 5A). Such fragments were used as controls. Second, a 90° similar cut was performed within the posterior compartment leaving a 3/4 regenerating fragment in which cells of the wound area do express bsk^{DN} (Fig. 5C). The GFP expression driven by *en* allowed both cuts to be done at a safe distance from the A/P compartment boundary. As expected, all (n = 11) 3/4 bsk^{DN} control fragments showed normal wound healing at 24 h (Fig. 5B). Instead, all 3/4 experimental fragments (n = 10) which expressed bsk^{DN} at the wound area were not healed (Fig. 5D). In all cases, the *en* pattern monitored by GFP was identical in control and experimental fragments. Statistical analysis using the Fisher exact test (Fisher, 1935) showed that there was a significant difference ($P < 0.05$) between bsk^{DN} control and experimental fragments. Finally, to check whether GFP overexpression or activation of the *Gal4/UAS* system might affect wound healing, 3/4 fragments from *en-Gal4*; *UAS-GFP* larvae were cut in similar ways as experimental discs and monitored. In all cases (n = 13), 3/4 fragments were healed at 24 h (Fig. 5E).

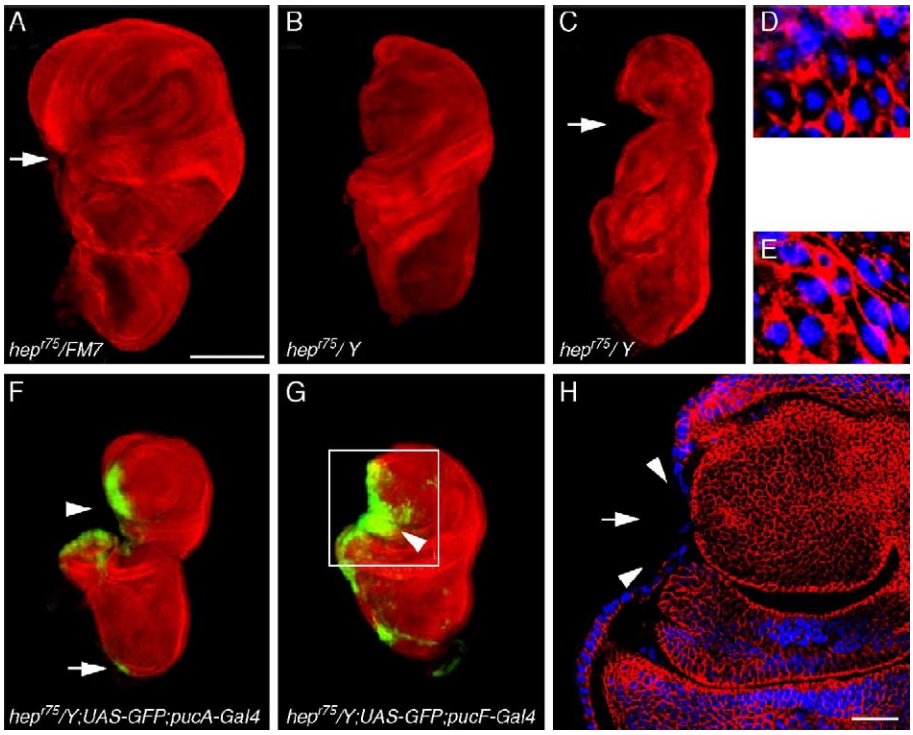

Fig. 4. Effect of *hemipterous* (*hep*) mutants and *puc* gene dosage on wound healing of imaginal discs. (A) 3/4 fragment of hep^{r75}/*FM7* larval females 24 h after in vivo culture shows an almost complete wound healing (arrow). (B) 3/4 fragment of hep^{r75}/*Y* larvae 24 h after in vivo culture shows a non-healed wound. (C) 3/4 fragment of hep^{r75}/*Y* larvae after 7 days of in vivo culture. Wound (arrow) remains non-healed and the fragment has not regenerated. (D, E) High magnification of PE cells from 3/4 fragments after 24 h of in vivo culture. PE cells in hep^{r75}/*Y* fragments (D) do not elongate towards the wound edge. In hep^{r75}/*Y;* $puc^{E69\text{-}F}$*-Gal4; UAS-GFP* fragments (E) elongation of PE cells is restored. (F) 3/4 fragment of hep^{r75}/*Y;* $puc^{E69\text{-}A}$*–Gal4;UAS-GFP* larvae after 24 h of culture. Wound is not healed though *puc* is expressed (green) at the wound edge (arrowhead). *puc* expression is reduced at the stalk (arrow). (G) 3/4 fragment of hep^{r75}/*Y;* $puc^{E69\text{-}F}$*-Gal4*;*UAS-GFP* larvae after 24h of in vivo culture. *puc* expression (green) spreads up to an average of 15–20 rows of CE cells (arrowhead) from the wound edge. (H) Enlargement of white square in (G). *puc* expression not shown. Wound tips curl to minimize the wound surface (arrowheads) and PE cells cover the vertex (arrow). For all images: fasciclin III (red), *hth* (blue) and *puc* (green). Scale bar in (A): 100 μm, (B, C, F, G) same scale. Scale bar in (H): 20 μm.

Dfos together with *bsk* are required downstream from *hep* for embryonic dorsal closure (Hou et al., 1997; Riesgo-Escovar and Hafen, 1997; Zeitlinger et al., 1997). However, it has been suggested that *Dfos* also responds to the ERK signaling pathway through phosphorylation sites different to those for the JNK response (Ciapponi et al., 2001). Therefore, we analyzed whether *Dfos* has a role in wound healing and whether ERK signaling pathway has also a significant role in such process. A similar experimental approach as for *bsk* function was set using three different classes of $Dfos^{DN}$ mutants (Ciapponi et al., 2001): $Dfos^{N\text{-}Ala}$ (bearing alanine substitutions at the JNK-specific phosphorylation sites), $Dfos^{C\text{-}Ala}$ (bearing alanine substitutions at the ERK-specific phosphorylation sites), and $Dfos^{Pan\text{-}Ala}$ (bearing alanine substitutions in all phosphorylation sites). *en-Gal4*; *UAS-GFP/UAS-*$Dfos^{DN}$ wing discs were cut out to produce control and experimental 3/4 regenerating fragments. (Fig. 6). Discs were monitored at 24 h of regeneration.

Experimental 3/4 regenerating fragments showed different degrees of healing (Figs. 6D–F). Whereas only 35% ($n = 20$) of $Dfos^{N\text{-}Ala}$ 3/4 fragments showed normal wound healing (Fig. 6D), more than 80% ($n = 26$) of $Dfos^{C\text{-}Ala}$ 3/4 fragments and 50% ($n = 12$) of $Dfos^{Pan\text{-}Ala}$ 3/4 fragments were almost healed at 24 h (Figs. 6E, F). Differences between $Dfos^{N\text{-}Ala}$ control and experimental fragments, between $Dfos^{Pan\text{-}Ala}$ control and experimental fragments, and between $Dfos^{N\text{-}Ala}$ and $Dfos^{C\text{-}Ala}$ experimental fragments were statistically significant ($P < 0.05$) using the Fisher exact test (Fisher, 1935). Instead, statistical differences were found not significant ($P > 0.05$) between $Dfos^{C\text{-}Ala}$ control and experimental fragments. Because $Dfos^{N\text{-}Ala}$ acts through the JNK, whereas $Dfos^{C\text{-}Ala}$ act through the ERK pathway, these results suggest a main role for the JNK pathway in this process, whereas the ERK pathway seems only to play a minor one. 3/4 control fragments of identical dominant negative forms of *Dfos* showed over 90% wound healing at 24 h (Figs. 6A–C). Overall, these results strongly support a specific role of *Dfos* in imaginal discs wound healing through JNK signalling pathway.

Inhibition of JNK signaling pathway and wound healing through overexpression of puc

The role of *puc* as a phosphatase downregulating the JNK pathway through *bsk* could be used to inhibit this pathway through *puc* overexpression. To carry it out, we used a similar system as for bsk^{DN} and $Dfos^{DN}$ overexpression. Wing discs from *en-Gal4*; *UAS-GFP/UAS-puc2A* were cut to produce

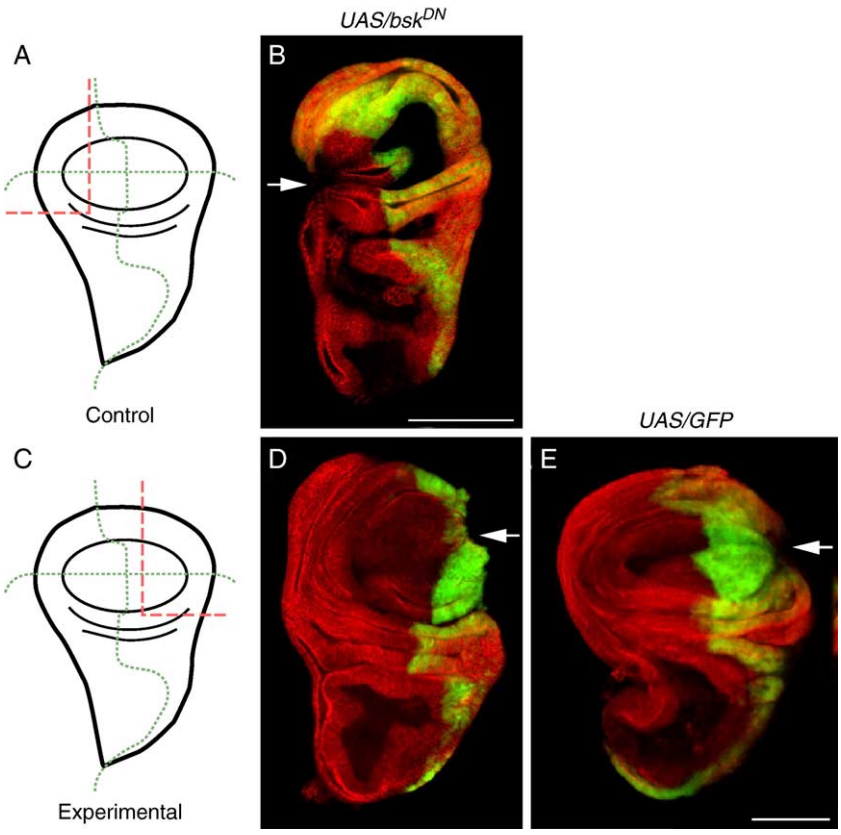

Fig. 5. Effects of bsk^{DN} mutants on wing imaginal disc wound healing. Double staining for *en* expression domain (green; *en-Gal4/UAS-GFP/UAS-bsk*^{DN}) and Fasciclin III (red) (A, C) schematic representations of 3/4 control (A) and 3/4 experimental (C) fragments showing the cutting lines (broken red lines) and the anteroposterior and dorsoventral compartment boundaries (dotted green lines). (B, D, E) wing discs fragments after 24 h of in vivo culture. Arrows point at the wound area. (B) 3/4 control fragment of an *en-Gal4; UAS-GFP/UAS-bsk*^{DN} wing disc showing a normal healing phenotype. (D) 3/4 experimental fragment of an *en-Gal4; UAS-GFP/UAS-bsk*^{DN} wing disc with an open wound phenotype. (E) 3/4 fragments not overexpressing bsk^{DN} (*en-Gal4; UAS-GFP*) show normal wound healing. In all figures, scale bars: 100 μm.

3/4 control and experimental fragments (see Fig. 5 for comparison). Whereas over 91% (n = 11) of all 3/4 control fragments bearing wound edges bounded by anterior compartment cells which do not overexpress *puc* healed normally (Fig. 7A), only 40% of 3/4 experimental fragments (n = 10) with wound edges bounded by posterior compartment cells overexpressing *puc* were healed at 24 h (Fig. 7B). Statistical analysis using the Fisher exact test (Fisher, 1935) showed that there was a mild but significant difference ($P < 0.05$) between control and experimental fragments. These results indicate that overproduction of *puc* slows down wound healing likely down-regulating the JNK signaling pathway.

Table 1 summarizes the percentages of healed and non-healed 3/4 control and experimental imaginal disc fragments, 24 h after cutting, under different genetic backgrounds.

Cell biology consequences of mutations in the JNK signalling pathway

On a cellular basis, wound healing of WT discs is accomplished through the formation of an actin-rich cable and filopodia for zipping epithelial edges together as well as by shape changes of the leading cells. Results so far reported also indicate that activation of the JNK signaling pathway is also necessary for proper wound healing and regeneration. Therefore, it should be expected that mutants of the JNK pathway block or reduce wound healing by inhibiting or slowing down the formation of the actin-rich cable and filopodia at the wound edges.

To test it, we used the mutant hep^{r75}/Y as well as the overexpression of bsk^{DN} because they have been shown to be the strongest inhibitors of wound healing (see Table 1). 3/4 fragments of both mutants were produced and stained for actin cytoskeleton with rhodamine-phalloidin to compare actin cable formation and the extent of filopodial protrusions with WT 3/4 fragments. At 5 h, hep^{r75}/Y 3/4 fragments showed only an actin-rich area at the wound vertex but not in the rest of the wound (Fig. 8A). This contrasts with the actin-rich cable seen all along the wound in WT fragments (Fig. 2A). The zippering process was also affected in hep^{r75}/Y 3/4 fragments. At 5 h, and even after 24 h (Fig. 8B), the wound remained wide open and the number of filopodial protrusions was much reduced when compared to control fragments (Figs. 2B–D). 3/4 fragments overexpressing bsk^{DN} show an actin-rich area at the wound vertex but

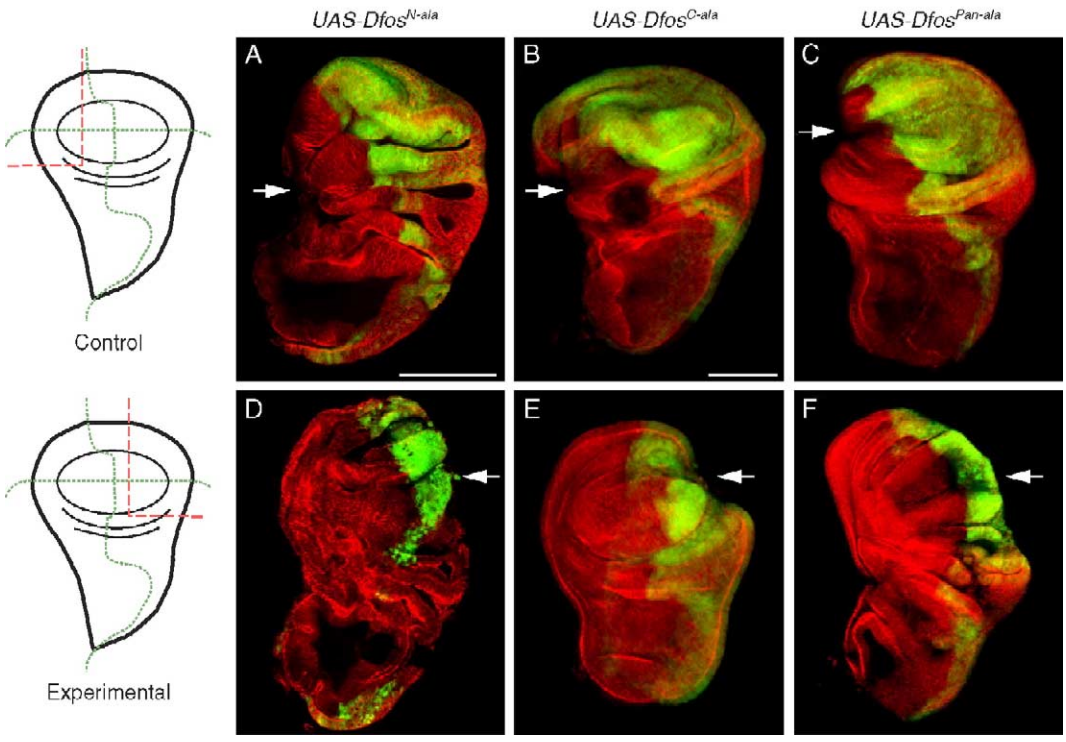

Fig. 6. Effects of *Dfos*^{DN} overexpression on imaginal disc wound healing. Arrows point to the wound area. Double staining for *en* expression domain (green; *en-Gal4/UAS-GFP/UAS-Dfos*^{DN}) and Fasciclin III (red). (A–C) 3/4 control fragments after 24 h of in vivo culture overexpressing three different dominant negative forms of *Dfos*: *Dfos*$^{N\text{-}Ala}$ (A), *Dfos*$^{C\text{-}Ala}$ (B), and *Dfos*$^{Pan\text{-}Ala}$ (C) within the posterior compartment. For all *Dfos*^{DN} forms, most fragments show closed wounds. (D–F) 3/4 experimental fragments at 24 h of in vivo culture overexpressing *Dfos*$^{N\text{-}Ala}$(D), *Dfos*$^{C\text{-}Ala}$ (E) and *Dfos*$^{Pan\text{-}Ala}$ (F). (D) and (F) do not show evidences of wound healing whereas the fragment in (E) is almost healed. In all figures, Fasciclin III is in red, and *en-GAL4; UAS-GFP/UAS-Dfos* in green. Scale bars: 100 μm.

not in the rest of the wound at 5 h of regeneration when cuts were made within the posterior compartment (Fig. 8D). Instead, 3/4 control fragments bearing wound edges within the anterior compartment, which do not overexpress bsk^{DN}, have a thick actin-rich cable all along the entire wound (Fig. 8C) as in regenerating WT discs (Fig. 2A).

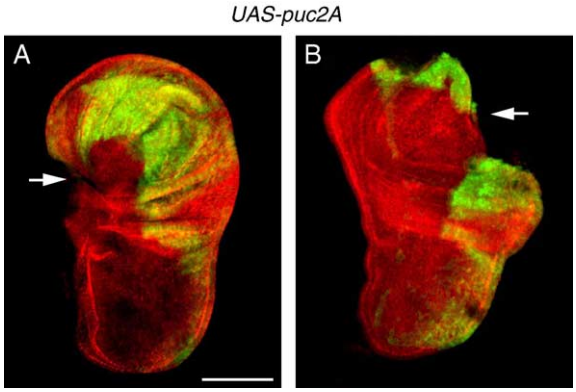

Fig. 7. Effects of *puc* overexpression on imaginal disc wound healing. Double staining for *en* expression domain (*en-Gal4/UAS-GFP/UAS-puc*; green) and Fasciclin III (red). (A) 3/4 control fragment after 24 h of in vivo culture showing an almost complete healed phenotype. Arrow points to the wound. (B) 3/4 experimental fragment 24 h after in vivo culture. 50% of fragments (see Table 1) remain non-healed. In all figures, scale bar: 100 μm.

Altogether, these results strongly suggest that mutants in the JNK signalling pathway inhibit or delay wound healing and regeneration by limiting the formation of the actin-rich cable and filopodial protrusions at the wound edge.

Discussion

All animal epithelia avoid empty spaces and have a strong tendency to restore their physical continuity following damage. The epithelia of *Drosophila* imaginal discs is not an exception to this rule. Here, we have examined the process of wound healing after cutting in wing imaginal discs and the role of the components of the JNK pathway in this process. In agreement with earlier reports, we observed that cell migration does not play a major role in initial healing. Instead, wound closure is carried out by contraction of cells of both epithelia (columnar and peripodial) around the wound. This allows connections to be made between epithelial cells at the vertex of the wound, which initiates a zippering process progressing from distal to proximal areas. In addition, this is the first report to our knowledge of the in vivo requirement of the *Drosophila* JNK signalling pathway in wound healing during regeneration

Table 1
Number and percentages oh healed wing disc fragments of different genotypes after 24 h of in vivo culture

Genotype	Fragment[a]	N[b]	Healed	% healed[c]
puc-Gal4; UAS-GFP	3/4	10	10	100
hep^{r75}/Y	3/4	14	0	0
hep^{r75}/FM7,GFP	3/4	14	12	86
en-Gal4; UAS-GFP	3/4	13	13	100
en-Gal4; UAS-GFP/UAS-bsk^{DN}	3/4 E	10	0	0
en-Gal4; UAS-GFP/UAS-bsk^{DN}	3/4 C	11	11	100
en-Gal4;UAS-GFP/UAS-puc2A	3/4 E	10	4	40
en-Gal4;UAS-GFP/UAS-puc2A	3/4 C	12	11	92
en-Gal4;UAS-GFP/UAS-Dfos$^{N\text{-}ala}$	3/4 E	20	7	35
en-Gal4;UAS-GFP/UAS-Dfos$^{N\text{-}ala}$	3/4 C	20	18	90
en-Gal4;UAS-GFP/UAS-Dfos$^{C\text{-}ala}$	3/4 E	26	21	81
en-Gal4;UAS-GFP/UAS-Dfos$^{C\text{-}ala}$	3/4 C	13	12	92
en-Gal4;UAS-GFP/UAS-Dfos$^{Pan\text{-}ala}$	3/4 E	12	6	50
en-Gal4;UAS-GFP/UAS-Dfos$^{Pan\text{-}ala}$	3/4 C	10	10	100

[a] 3/4, 3/4 control (3/4 C), and 3/4 experimental (3/4 E) indicate the three types of fragments produced. For further details, see Material and methods and legends of Figs. 1 and 5.
[b] Number of fragments analyzed.
[c] Percentages have been rounded to the nearest integer.

of imaginal discs. These results bear interesting parallels to those of other morphogenetic processes in *Drosophila* and other organisms.

Wound healing in imaginal discs

In most examples of closing and healing in epithelia other than imaginal discs, cells spread or migrate over a substrate or are dragged by push and pull forces to close epithelial discontinuities. Common substrates are the basal lamina, plugs of hemocytes (Bohn, 1975; Wigglesworth, 1937), and a plethora of different mesodermal or mesenchymal cell types (Martin, 1997; Pedersen, 1976). In *Drosophila*, well-studied examples of substrates are the larval cells in disc thoracic closure (Agnès et al., 1999; Noselli and Agnès, 1999; Pastor-Pareja et al., 2004), and a melanin clot and some undisclosed cells and cell debris in embryo, larval, and adult wound healing (Galko and Krasnow, 2004; Rämet et al., 2002; Wood et al., 2002). In turn, the amnioserosa cells are instrumental exerting pulling forces during embryonic dorsal closure (Glise and Noselli, 1997; Jacinto et al., 2000, 2002; Martin-Blanco et al., 1998). Likely, interactions between spreading cells and substrate cells should play a substantial role during closure and healing.

In the absence of substrate, cells of the CE and PE in disc fragments should rely on mechanisms other than migration, spreading, and pushing/pulling forces to close the wound. As first described by Reinhard et al. (1977), the wound

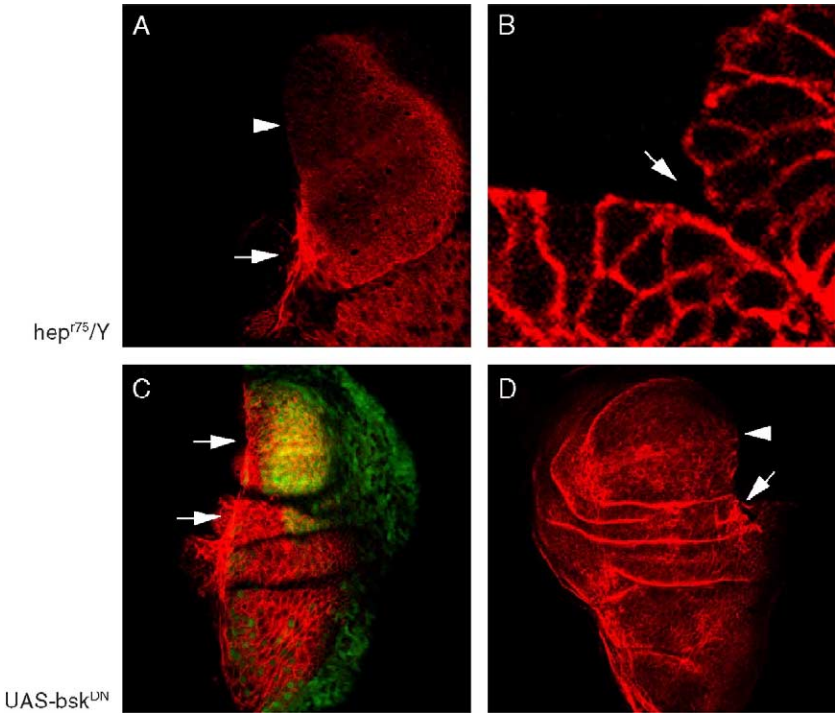

Fig. 8. Effects of the JNK mutants *hemipterous* (*hep^{r75}*; A, B) and *basket* (*UAS-bsk^{DN}*; C, D) on the actin cytoskeleton and filopodial extensions (stained with phalloidin, red) during wound healing. (A) Projection of PE confocal planes at the wound edge of a 3/4 fragment of *hep^{r75}/Y* after 5 h of culture. The actin-rich cable (arrow) covers a limited range of the wound (arrowhead) as compared to wild type 3/4 fragments (see Fig. 2A for comparison). (B) Detail of a confocal plane at the CE of a 3/4 fragment of *hep^{r75}/Y* imaginal disc after 24 h. The wound remains wide open and the number of filopodia at the wound vertex (arrow) is very small compared to wild type 3/4 fragments (see Figs. 2B–D for comparison). (C, D) PE confocal planes of 3/4 control and experimental fragments, respectively, of *en-Gal4; UAS-GFP/UAS-bsk^{DN}* larvae. GFP (green) delineates the posterior compartment. To enhance the cytoskeleton, GFP expression in D is not shown. (C) 3/4 control fragments after 5 h of in vivo culture. An actin cable is clearly seen all along the wound (arrows). (D) 3/4 experimental fragment after 5 h of in vivo culture. The actin cable is only observed at the wound vertex (arrow) and does not span the whole area of the wound (arrowhead).

surfaces of both epithelia curl over towards the lumen. Such curling likely results from contraction of the actin-rich cable at the apical end of border cells of the wound. This cable, present in both epithelia, is more apparent along the wound edge of the PE and at the vertex areas of both epithelia (Fig. 2A). In both epithelia, contraction of the actin cable induce subsequent changes in the overall morphology of disc fragments, which is already apparent 5 h after cutting (Fig. 9B) and specially at 12 h (Fig. 9C). The second driving force is exerted through filopodial extensions already present along the wound area soon after cutting. At the vertex, such extensions allow contacts between cells which start the zippering process by pulling and knitting wound edges together (Figs. 2B–D; 9E). This process seems to proceed from proximal (central) to distal (peripheral) areas of the disc until the wound is closed. At the cellular level, zipping appear to start from filopodia at the basal–lateral border of cells at the wound edge, the apical part lagging behind in time (Figs. 1E, G, I). This proximal–distal, basal–apical, zippering process is completed at 24 h (Fig. 9D). Similar to embryonic dorsal closure (Jacinto et al., 2002), the actin cable might also restrict an excess of activity of filopodia in imaginal disc wound healing maintaining a smooth edge for a more efficient zippering. However, this remains to be tested.

Altogether, these observations suggest that healing of wing imaginal discs is completed by a "purse-string" contraction of the actin cable together with cellular zippering by filopodial extension and adhesion. In contrast, neither in larval and adult experimental wound healing (Galko and Krasnow, 2004; Rämet et al., 2002), a multicellular actin cable indicative of the "purse-string" closure

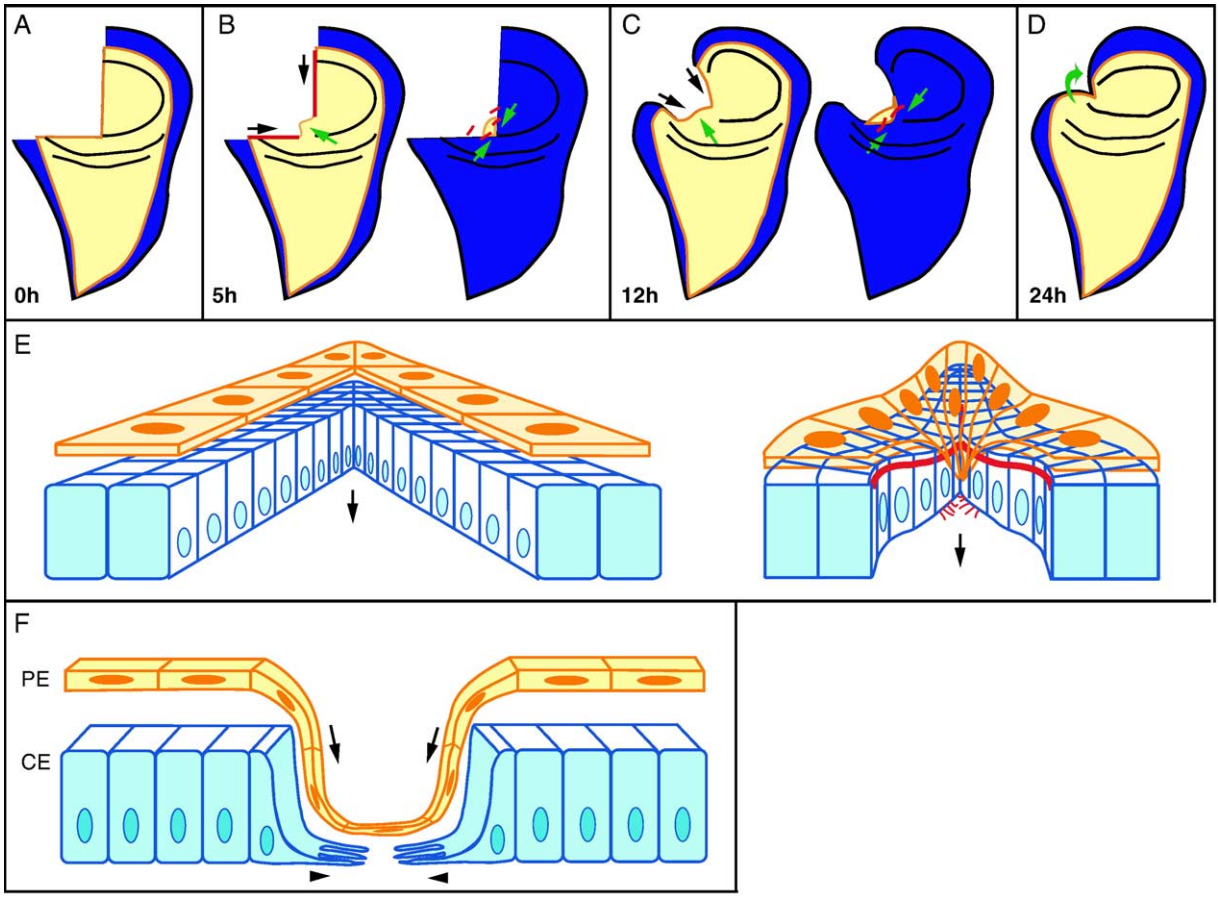

Fig. 9. A tentative model of wound healing in imaginal discs. (A) Schematic PE view of a 3/4 wing disc fragment soon after cutting. CE is shown in dark blue and PE in orange. (B) 5 h after cutting. Left, PE view. An actin cable forms at the edge of the PE (red lines, left) pulling in the wound edges (black arrows) shrinking the wound surface. PE cells elongate towards the wound vertex (green arrow). Right, CE view. CE cells extend filopodial processes (red lines) to zip wound cells at the vertex. (C) 12 h after cutting. Left, PE view. Increasing numbers of PE cells elongate towards the wound vertex (green arrow) pulling in the wound edges (black arrows). Right, CE view. PE cells still cover the wound vertex, whereas filopodial processes (red lines) progressively zipper the wound (green arrows). (D) PE view of a 3/4 wing disc fragment 24 h after cutting. Wound healing is completed with PE cells covering the healed region (arrow). (E) Schematic frontal views of the wound vertex soon after cutting (left) and during the zippering process (right). The wound closes (black arrows) from inside (distal) to outside (proximal) due to the contraction of the apical actin supercable (thick red lines in the CE) and filopodial extensions (basal thin red lines). PE cells (orange) help wound healing elongating towards the wound and covering the vertex. (F) Schematic representation of a Z section at the wound vertex. PE (orange) elongates down covering the wound vertex (arrows), whereas CE cells (blue) extend filopodial processes from their basal–lateral surfaces (arrowheads) knitting the CE cells at the wound edge.

mechanism as described in embryonic wound healing (Wood et al., 2002) has been observed or reported in the spreading cells. Moreover, although both "purse-string" contraction and filopodial extension do occur in embryonic wound healing, either alone can drive wound closure as shown through modulation of the activities of the small GTPases *Rho* and *Cdc42* (Wood et al., 2002).

Further testing of the proposal set in Fig. 9 for imaginal disc wound healing would be to analyze in real time wound healing in cultured disc fragments using suitable markers and to study in depth the role of the PE.

The role of the JNK pathway during imaginal disc wound healing

Components of the JNK pathway (Fig. 3A) seem to be required for optimal wound healing during regeneration. First, *puckered* (*puc*), a specific transcriptional target of the JNK pathway, is specifically induced in CE and PE cells at the edge of the wound in regenerating wing discs (Figs. 3D–H). Second, *puc* gene induction (starting at 4–5 h after cutting) correlates in time and space with changes in cell shape (elongation of peripodial cells). Such changes are at his height (12–24 h) when *puc* expression is maximal in number of cells and spatial range (Figs. 3J, K). Third, embryonic dorsal closure, disc thoracic closure, and larval and adult wound healing are morphologically similar to imaginal wound healing in that they also rely on JNK activation to control *puc* gene expression in epithelial cells. Accordingly, we found that wound healing during regeneration fails to initiate or is aberrant in different mutants of the JNK pathway. This strongly supports a key role for this pathway in the process of wound closure.

One of the upstream regulators of the JNK pathway, the gene *hemipterous* (*hep*), which encodes a MAPKK, was the first reported to cause large holes in the dorsal cuticle resulting in embryonic lethality (Glise et al., 1995). Similarly, regenerating discs from hemizygous *hep* mutants, remain unhealed after 7 days. In these discs, *puc* expression is strongly reduced at the wound confirming the role of *hep* on the activation of *puc* (Fig. 4F). However, *puc* is a MAPK phosphatase that operates as a negative regulator of the JNK pathway acting on the MAPK gene *basket* (*bsk*). Therefore, *hep* and *puc* have opposite effects. As such, the unhealed phenotype of regenerating discs mutant for *hep* should be rescued in flies with lower than normal copies of puc^{+}. Indeed, hep^{r75}/Y fly mutant discs carrying one dose of puc^{+} rescued the *hep* phenotype (Figs. 4G, H) showing partial healing, whereas hep^{r75}/Y flies carrying two copies of puc^{+} showed no rescue and non-healing phenotypes (Fig. 4F). Conversely, it should also be expected that overexpression of *puc* should inhibit wound healing through inhibition of JNK pathway. *UAS-puc2A* driven by *en-Gal4* within the posterior compartment showed that 3/4 fragments with wound edges belonging to posterior *puc* overexpressing cells do not heal, whereas those with wound boundaries belonging to anterior non-expressing *puc* healed (Fig. 7). Altogether, these results indicate that *puc* expression needs to be finely tuned for proper wound healing to occur.

Moreover, components of the JNK pathway downstream of *hep* but upstream of *puc* should also be active during imaginal disc wound healing. In embryonic dorsal closure, disc thoracic closure and adult wound healing, *bsk*, *Djun*, and *Dfos* are required to complete these processes. We tested its function during wound healing overexpressing UAS dominant negative forms of *bsk* and *Dfos* in the posterior compartment driven by *en-Gal4*. As expected, fragments whose wound edge cells belong to the posterior compartment expressing $UAS\text{-}bsk^{DN}$ did not heal, whereas those fragments with wound edge cells belonging to the anterior compartment, which do not express $UAS\text{-}bsk^{DN}$, healed normally (Fig. 5). UAS-dominant negative JNK specific forms of *Dfos* ($UAS\text{-}Dfos^{N\text{-}Ala}$) showed similar, albeit not so strong, results. Instead, only mild effects appear with ERK specific dominant negative *Dfos* ($UAS\text{-}Dfos^{C\text{-}Ala}$), suggesting that similarly to disc thoracic closure (Ciapponi et al., 2001) *Dfos* acts in wound healing mainly through the JNK pathway, ERK pathway apparently playing only a minor role.

Altogether, these results point out that all components of the JNK pathway tested here are necessary for normal wound healing during imaginal disc regeneration. Moreover, as in embryonic dorsal closure and disc thoracic closure, the interplay between *hep*, *bsk*, *Dfos*, and *puc* also operates during imaginal disc wound healing.

The likely linkage between disruption of the actin cable and filopodia formation and inactivation or down-regulation of the JNK signalling pathway was analyzed in detail for 3/4 fragments discs of hep^{r75}/Y and bsk^{DN} mutant backgrounds (Fig. 8). Both showed clear reductions in the actin-rich cable at the wound, now restricted to the wound vertex (Figs. 8A, D). Such reduction might likely inhibit the "purse-string" mechanism, operating by contraction of the actin cable, giving rise to open wounds (see 3/4 fragment of hep^{r75}/Y at 7 days of regeneration in Fig. 4C). In addition, the number of filopodia is also clearly reduced for both mutations (Fig. 8B for hep^{r75}/Y, and bsk^{DN} (not shown)) when compared to regenerating WT fragments (see Figs. 2B, C for comparison). Altogether, this strongly suggests that abnormal wound healing in mutant backgrounds for members of the JNK signalling pathway are a consequence of the lack of a proper actin-rich cable along the wound as well as of an insufficient number of filopodial extensions at the wound vertex. Both results into a lack of a proper "purse-string" mechanism to contract the wound and to halting or slowing down the zippering of the opposing epithelia.

Similarities and differences between adult and imaginal wound healing and other healing processes

Despite wound healing in regeneration of imaginal discs relies on the JNK signaling pathway as embryonic

dorsal closure, disc thoracic closure, and larval and adult wound healing do, some differences among them are worth mentioning. First and foremost, wound healing in discs do not involve cell migration and spreading above a substrate or push and pull forces. In contrast, JNK signaling is downregulated in amnioserosa cells prior to embryonic dorsal closure. Later on, it is upregulated when closure is near to be completed which results in contraction of amnioserosa cells which pull dorsalwards the epidermal cells connected to them (Reed et al., 2004). JNK activity persists in the leading edge of epithelial cells (Reed et al., 2001; Ricos et al., 1999) where *hep* activity induces *decapentaplegic* (*dpp*) which binds in paracrine and autocrine manner to epithelial cells to promote their own migration. In striking contrast with embryonic dorsal closure, *dpp* expression appears not to be under the control of *hep* in disc thoracic closure (Agnès et al., 1999). However, *dpp* and *puc* are co-expressed in the peripodial epithelium of discs undergoing thoracic closure, which suggests that the JNK and *dpp* pathways may also cooperate there. In adult wound healing, *dpp* is also not upregulated at the leading edge (Rämet et al., 2002).

A second difference between wound healing during regeneration and embryonic dorsal closure, disc thoracic closure, and larval and adult wound healing, refers to the spatial range of *puc* expression. During embryonic dorsal closure *puc* gene expression remains restricted to one row of the most dorsal epidermal cells. Instead in disc thoracic closure and larval and adult wound healing *puc* is expressed in several rows of cells. Such differences have been linked to the longer distances spanned by migrating cells in disc thoracic closure and adult wound healing compared to embryonic dorsal closure (Rämet et al., 2002). Similar to adult disc thoracic closure and adult wound healing, *puc* expression in disc wound healing follows a similar time course starting a few hours after cutting, peaking at 12 h, and decreasing from 18 h on. Interestingly, as it is the case in disc thoracic closure, and larval and adult wound healing, *puc* is also expressed in several rows of cells in imaginal disc wound healing. The extent of *puc* expressing area in regenerating imaginal discs might be related, like in adult wound healing, to the extent of the wound. This could be tested in regenerating discs bearing wounds of different sizes. Moreover, in adult wound healing *puc* is expressed in a decreasing gradient from the edge of the wound towards the healthy epithelium. Again, this remains to be studied in regenerating discs.

How is *puc* activated during wound healing and how its spatial and temporal expression time course are regulated? It has been suggested that factors released from the wound hyperactivate the JNK of cells close to it while *puc* phosphatase activity may not be sufficient to restrict JNK activity to the first row of cells at the wound edge (Rämet et al., 2002). Hence, several rows of cells would express *puc*. Indeed, in imaginal discs wound healing *puc* enhanced activity increases in *puc* mutant backgrounds or when a single copy of *puc* is present leading to a wider area of *puc* expressing cells (Fig. 4G). As in disc thoracic closure and adult wound healing, the broader range of cells (10–15 rows on average) in imaginal discs expressing *puc* at the wound compared to the 8 rows or so of cells in adult wound healing may be due to more extensive epithelial movements needed to close the wound in regenerating 3/4 fragments.

In conclusion, wound healing in regenerating imaginal discs of *Drosophila* represent a new and powerful model, to be added to the current models of embryonic dorsal closure, disc thoracic closure, and embryonic, larval, and adult wound healing, to understand how different signalling pathways participate and interact with the cytoskeletal machinery to generate complex morphogenetic processes. Wound healing in imaginal discs has an additional bonus: it is the first step to the ensuing process of regeneration. Therefore, wound healing could be used to address how it relates to regeneration, namely whether complete healing is needed to activate DNA synthesis and mitosis, whether extensive cell apoptosis is needed for regeneration to go on, and how cell–cell interactions during healing are instrumental to set pattern formation. These problems will be dealt with in a forthcoming series of papers.

Acknowledgments

We thank D. Bohman for *UAS-bsk*^{DN}, and R. Mann for anti-*hth*. We wish to thank A. García-Bellido and members of his lab for introducing MB into the main methods and techniques of imaginal disc manipulation and transplantation. The help of C. Arenas in statistical analyses is acknowledged. We would like to thank the referees for insights and suggestions which much helped to improve the manuscript. MB was a recipient of a PhD grant from the University of Barcelona. JB and FS are funded by grants from the Ministerio de Ciencia y Tecnologia and the Generalitat de Catalunya. EMB is funded from DGICYT, Ministerio de Educación y Ciencia.

References

Adler, P.N., 1984. DNA replication and pattern regulation in the imaginal wing disc of *Drosophila*. Dev. Biol. 102, 300–308.

Agnès, F., Suzanne, M., Noselli, S., 1999. The *Drosophila* JNK pathway controls the morphogenesis of imaginal discs during metamorphosis. Development 126, 5453–5462.

Bohn, H., 1975. Growth-promoting effect of haemocytes on insect epidermis in vitro. J. Insect Physiol. 21, 1283–1293.

Brand, A.H., Perrimon, N., 1993. Targeted gene expression as a means of altering cell fates and generating dominant phenotypes. Development 118, 401–415.

Bryant, P.J., 1975. Pattern formation in the imaginal wing disc of *Drosophila melanogaster*: fate map, regeneration and duplication. J. Exp. Zool. 193, 49–77.

Bryant, P.J., Fraser, S.E., 1988. Wound healing, cell communication, and

DNA synthesis during imaginal disc regeneration in *Drosophila*. Dev Biol. 127, 197–208.
Bryant, S.V., French, V., Bryant, P.J., 1981. Distal regeneration and symmetry. Science 212, 993–1002.
Ciapponi, L., Jackson, D.B., Mlodzik, M., Bohmann, D., 2001. *Drosophila* Fos mediates ERK and JNK signals via distinct phosphorylation sites. Genes Dev. 15, 1540–1553.
Dale, L., Bownes, M., 1981. Is regeneration in *Drosophila* the result of epimorphic regulation? Wilhelm Roux's Arch. Dev. Biol. 189, 91–96.
Dale, L., Bownes, M., 1985. Pattern regulation in fragments of *Drosophila* wing discs which show variable wound healing. J. Embryol. Exp. Morphol. 85, 95–109.
Dunne, J.F., 1981. Growth dynamics in the regeneration of a fragment of the wing imaginal disc of *Drosophila melanogaster*. Dev Biol. 87, 379–382.
Ferretti, P., Geraudie, J. (Eds.), 1998. Cellular and Molecular Basis of Regeneration. From Invertebrates to Humans. John Wiley and Sons, Chichester.
Fisher, R.A., 1935. The logic of inductive inference. J.R. Stat. Soc. Ser. A 98, 39–54.
French, V., Bryant, P.J., Bryant, S.V., 1976. Pattern regulation in epimorphic fields. Science 193, 969–981.
Galko, M.J., Krasnow, M.A., 2004. Cellular and genetic analysis of wound healing in *Drosophila* larvae. PloS Biol. 2 (8), e239.
Glise, B., Noselli, S., 1997. Coupling of Jun amino-terminal kinase and Decapentaplegic signaling pathways in *Drosophila* morphogenesis. Genes Dev. 11, 1738–1747.
Glise, B., Bourbon, H., Noselli, S., 1995. Hemipterous encodes a novel *Drosophila* MAP kinase kinase, required for epithelial cell sheet movement. Cell 83, 451–461.
Hou, X.S., Goldstein, E.S., Perrimon, N., 1997. *Drosophila* Jun relays the Jun amino-terminal kinase signal transduction pathway to the Decapentaplegic signal transduction pathway in regulating epithelial cell sheet movement. Genes Dev. 11, 1728–1737.
Jacinto, A., Wood, W., Balayo, T., Turmaine, M., Martinez-Arias, A., Martin, P., 2000. Dynamic actin-based epithelial adhesion and cell matching during *Drosophila* dorsal closure. Curr. Biol. 10, 1420–1426.
Jacinto, A., Wood, W., Woolner, S., Hiley, C., Turner, L., Wilson, C., Martinez-Arias, A., Martin, P., 2002. Dynamic analysis of actin cable function during *Drosophila* dorsal closure. Curr. Biol. 12, 1245–1250.
Karlsson, J., Smith, R.J., 1981. Regeneration from duplicating fragments of the *Drosophila* wing disc. J. Embryol. Exp. Morphol. 66, 117–126.
Martin, P., 1997. Wound healing—aiming for perfect skin regeneration. Science 276, 75–81.
Martin-Blanco, E., Gampel, A., Ring, J., Virdee, K., Kirov, N., Tolkovsky, A.M., Martinez-Arias, A., 1998. puckered encodes a phosphatase that mediates a feedback loop regulating JNK activity during dorsal closure in *Drosophila*. Genes Dev. 12, 557–570.
Meinhardt, H., 1983. Cell determination boundaries as organizing regions for secondary embryonic fields. Dev. Biol. 96, 375–385.
Noselli, S., Agnès, F., 1999. Roles of the JNK signaling pathway in *Drosophila* morphogenesis. Curr. Opin. Genet. Dev. 9, 466–472.
Pastor-Pareja, J.C., Grawe, F., Martín-Blanco, E., García-Bellido, A., 2004. Invasive cell behaviour during *Drosophila* imaginal disc eversion is mediated by the JNK signalling cascade. Dev. Cell 7, 387–399.
Pedersen, K.J., 1976. Scanning electron microscopical observations on epidermal wound healing in the planarian Dugesia tigrina. Wilhelm Roux's Arch. Dev. Biol. 179, 251–273.
Rämet, M., Lanot, R., Zachary, D., Manfruelli, P., 2002. JNK signaling pathway is required for efficient wound healing in *Drosophila*. Dev. Biol. 241, 145–156.
Reed, B.H., Wilk, R., Lipshitz, H.D., 2001. Downregulation of Jun kinase signaling in the amnioserosa is essential for dorsal closure of the *Drosophila* embryo. Curr. Biol. 11, 1098–1108.
Reed, B.H., Wilk, R., Schök, F., Lipshitz, H.D., 2004. Integrin-dependent apposition of *Drosophila* extraembryonic membranes promotes morphogenesis and prevents anoikis. Curr. Biol. 14, 372–380.
Reinhardt, C.A., Bryant, P.J., 1981. Wound healing in the imaginal discs of *Drosophila*: II. Transmission electron microscopy of normal and healing wing discs. J. Exp. Zool. 216, 45–61.
Reinhardt, C.A., Hodgkin, N.M., Bryant, P.J., 1977. Wound healing in the imaginal discs of *Drosophila*: I. Scanning electron microscopy of normal and healing wing discs. Dev. Biol. 60, 238–257.
Ricos, M.G., Harden, N., Sem, K.P., Lim, L., Chia, W., 1999. Dcdc42 acts in TGF-beta signaling during *Drosophila* morphogenesis: distinct roles for the Drac1/JNK and Dcdc42/TGF-beta cascades in cytoskeletal regulation. J. Cell Sci. 112, 1225–1235.
Riesgo-Escovar, J.R., Hafen, E., 1997. *Drosophila* Jun kinase regulates expression of decapentaplegic via the ETS-domain protein Aop and the AP-1 transcription factor DJun during dorsal closure. Genes Dev. 11, 1717–1727.
Schubiger, G., 1971. Regeneration, duplication and transdetermination in fragments of the leg disc of *Drosophila melanogaster*. Dev. Biol. 26, 277–295.
Schubiger, G., 1973. Regeneration of *Drosophila melanogaster* male leg disc fragments in sugar fed female hosts. Experientia 29, 631–632.
Ursprung, H., 1967. In vivo culture of *Drosophila* imaginal discs. In: Wilt, F.H., Wessels, N.K. (Eds.), Methods in Developmental Biology. T.Y. Crowell, New York, pp. 485–492.
Wigglesworth, V.B., 1937. Wound healing in an insect (*Rhodnius prolixus* Hemiptera). J. Exp. Biol. 14, 364–381.
Wood, W., Jacinto, A., Grose, R., Woolner, S., Gale, J., Wilson, C., Martin, P., 2002. Wound healing recapitulates morphogenesis in *Drosophila* embryos. Nat. Cell Biol. 4, 907–912.
Zeitlinger, J., Bohmann, D., 1999. Thorax closure in *Drosophila*: involvement of Fos and the JNK pathway. Development 126, 3947–3956.
Zeitlinger, J., Kockel, L., Peverali, F.A., Jackson, D.B., Mlodzik, M., Bohmann, D., 1997. Defective dorsal closure and loss of epidermal decapentaplegic expression in *Drosophila* fos mutants. EMBO J. 16, 7393–7401.